Detection of a variable intracellular acid-labile carbon pool in Thalassiosira weissflogii (Heterokontophyta) and Emiliania huxleyi (Haptophyta) in response to changes in the seawater carbon system

Journal:	*Physiologia Plantarum*
Manuscript ID:	Draft
Manuscript Type:	Regular manuscript - Biochemistry and metabolism
Date Submitted by the Author:	n/a
Complete List of Authors:	Isensee, Kirsten; University Oviedo, Biologia; UNESCO/IOC, Ocean Science Section Erez, Jonathan; The Hebrew University in Jerusalem, Earth Science Institute St, Heather; University Oviedo, Geologia
Key Words:	Carbon pool, diatom, coccolithophorid, inorganic carbon uptake, disequilibrium method

Detection of a variable intracellular acid-labile carbon pool in *Thalassiosira weissflogii* (Heterokontophyta) and *Emiliania huxleyi* (Haptophyta) in response to changes in the seawater carbon system

Kirsten Isensee[1,2*], Jonathan Erez[3], and Heather M. Stoll[1]

1) Dept. de Geologia, Universidad Oviedo, 33006 Oviedo, Asturias, Spain

2) Now at: Intergovernmental Ocean Comission, UNESCO, 1 rue Miollis 75732 Paris cedex 15 France

3) Jonathan Erez, The Hebrew University of Jerusalem, The Institute of Earth Sciences, Edmond Safra Campus, Givat Ram, Jerusalem 91904, Israel

*Corresponding author, k.isensee@gmail.com.

ABSTRACT

Accumulation of an intracellular pool of carbon (C_i pool) is one strategy by which marine algae overcome the low abundance of dissolved CO_2 ($CO_{2(aq)}$) in modern seawater. To identify the environmental conditions under which algae accumulate an acid-labile C_i pool, we applied a ^{14}C pulse-chase method, used originally in dinoflagellates, to two new classes of algae, coccolithophorids and diatoms. This method measures the carbon accumulation inside the cells without altering the medium carbon chemistry or culture cell density. We found that the diatom *Thalassiosira weissflogii* ((Grunow) G.Fryxell & Hasle) and a calcifying strain of the coccolithophorid *Emiliania huxleyi* ((Lohmann) W.W.Hay & H.P.Mohler) develop significant acid-labile C_i pools. Ci pools are measureable in cells cultured in media with 2 to 30 µmol L^{-1} $CO_{2(aq)}$, in these cultures corresponding to a medium pH of 8.6 -7.9. The absolute C_i pool was greater for the larger-celled diatoms. For both algal classes the C_i pool became a negligible contributor to photosynthesis once $CO_{2(aq)}$ exceeded 30 µmol L^{-1}. Combining the ^{14}C pulse-chase method and ^{14}C disequilibrium method enabled us to assess whether *E. huxleyi* and *T. weissflogii* exhibited thresholds for foregoing accumulation of DIC or reduced the reliance on bicarbonate uptake with increasing $CO_{2(aq)}$. We showed that the C_i pool decreases with higher CO_2:HCO_3^- uptake rates.

Abbreviations

α_1, α_2, temperature, salinity and pH dependent first order rate constants for CO_2 and hydration; AA, added activity; C, carbon; CA, chase activity; CCF, carbon concentration factor; CCM, carbon concentration mechanism; CF, chase filter; Chl*a*, chlorophyll a; C_i pool, intracellular pool of acid-labile carbon; CPM, counts per minute; D, dark; DBS, dextran bound sulfonamide; DIC, dissolved inorganic carbon; DPM, desintegrations per minute; eCA, extracellular carbonic anhydrase; *f*, fraction of DIC uptake attributable to HCO_3^-; iCA, intracellular carbonic anhydrase; L, light; LD, light:dark; MIMS, membrane inlet mass spectrometry; P+C, pulse chase method; PEPC, phosphoenolpyruvate carboxylase; ΔSA_{CO2}, difference between initial and equilibrium values of specific CO_2 activity;ΔSA_{HCO3}, difference between initial and equilibrium values of specific HCO_3^- activity; SA_{DIC}, specific activity of dissolved inorganic carbon at equilibrium; SOC, silicon oil centrifugation method; SW, seawater; t, time; TZ, time zero; V_t, total rate of DIC uptake

INTRODUCTION

In modern seawater, the ambient concentration of dissolved inorganic carbon (DIC) in the form of uncharged carbon dioxide ($CO_{2(aq)}$) varies between 10 and 15 µmol L^{-1} at a pH ~ 8.05. $CO_{2(aq)}$ is the required substrate of the enzyme RubisCO, which is responsible for the major part of carbon (C) fixation in the biosphere. This ancient highly conserved protein not only plays a central, but also limiting role during photosynthetic C assimilation, due to its catalytic inefficiency under modern atmospheric conditions (low CO_2 and high O_2 concentrations). Because it evolved in an atmosphere with nearly 20 fold higher $CO_{2(aq)}$ levels compared to the present concentration (e.g. Tortell 2000), the poor catalytic efficiency hampers maximum carbohydrate production (K_M of 20-70 µmol L^{-1}, (Badger et al. 1998)). Consequently, at present $CO_{2(aq)}$ concentrations marine algae have to enrich CO_2 actively at the catalytic site of RubisCO via operating carbon concentrating mechanisms (CCMs).

During the last several decades, the diversity of CCMs in marine microorganisms and the variable efficiencies of different RubisCO enzyme types have been elucidated by a variety of methods(e.g. Badger et al. 1998, Giordano et al. 2005, Kaplan et al. 1980, Kaplan and Reinhold 1999, Roberts et al. 2007). An essential component of CCMs is an active influx of inorganic C across the cell membrane (Raven 1995). The active uptake of DIC across the plasmalemma and the hydration of CO_2 inside the cytoplasm can result in enhanced intracellular DIC concentrations compared to the DIC concentrations in the medium (Badger et al. 1998), although CCMs do not necessarily result in an accumulation of inorganic C inside the cell, because of direct transfers of DIC to catalytic site of RubisCO. Several recent studies suggest that the most effective CCMs are those which rely on enhancement of DIC (or DIC-organic complexes) in the cell while maintaining cytoplasm CO_2 concentrations which are not significantly elevated with respect to those of seawater to avoid strong leakage of CO_2 through the cell membrane (e.g. Cassar et al., 2006, Hopkinson et al., 2011). In these

models, C is transported from the cytoplasm to the chloroplast as HCO_3^-, and only within the chloroplast or pyrenoid region at the site of RubisCO, converted to CO_2. Likely, an intracellular carbonic anhydrase (iCA) is important in this conversion into CO_2 (e.g. Giordano et al. 2005, Raven 2010, Trimborn et al. 2009). Alternatively, in some marine diatoms, C may be transported from the cytoplasm to the site of photosynthesis as a C_4 compound (Morel et al. 2002, Reinfelder et al. 2000, Roberts et al. 2007). In addition, some algae species exhibit high extracellular carbonic anhydrase (eCA) activities, which catalyzes the equilibrium replenishment from seawater of $CO_{2(aq)}$ or bicarbonate (HCO_3-) and minimizes depletion of CO_2 in the cell´s boundary layer (Aizawa and Miyachi 1986, Berman-Frank et al. 1994, Spalding et al. 1983, Trimborn et al. 2008).

Yet, the operation of CCMs comes at some energetic cost to the organism. The formation and maintenance of CCMs requires light energy as well as nutrients to make the key proteins for these reactions. These costs of the different types of CCMs may play a role in competitive interactions among taxa in the modern ocean in their biogeography and seasonal succession (Tortell 2000). Due to the high impact of CCMs on the energetic metabolism and physiology of the cells, it is of particular interest to examine experimentally, if CCMs are reduced at higher concentrations of $CO_{2(aq)}$, whether two species belonging to different algal classes reduce the size of C_i pools at similar thresholds of $CO_{2(aq)}$ and how this influences algae growth. C acquisition strategies of algae may be characterized by assessing the degree of accumulation of intracellular C, the proportion of each species of C (HCO_3^- or CO_2) used for photosynthesis, and the fluxes of each substrate into and out of the cell. Other characterizations include expression of key enzymes involved in CCMs, such as iCA and eCA or phosphoenolpyruvate carboxylase (PEPC).

In this study, we concentrate on the existence and significance of intracellular C accumulation, considering total accumulation in the cell and considering the full acid-labile C_i

pool which subsequently contributes to photosynthesis. We employ a ^{14}C pulse-chase method which indirectly determines the C_i pools contributing to photosynthesis, and compare the size of the C_i pool at varying pH values and $CO_{2(aq)}$ of two different microalgae species, a coccolithophorid and a diatom. This pulse-chase method was first described by ter Kuile and Erez (1987, 1988) for measuring the C_i pools of benthic foraminifera, and was later used to characterize the C_i pool of dinoflagellates (Berman-Frank and Erez 1996) and brown macroalgae (Johnston 1991). The pulse-chase method distinguishes the cellular content of acid-labile forms of C, which include free CO_2, HCO_3^- and CO_3^{-2} as well as C that may be bound or complexed to organic molecules. The fraction of this acid-labile C which is subsequently incorporated into acid-stable forms via photosynthesis, is defined as the intracellular C (C_i) pool. In this work, we extend the use of the pulse-chase method to two new algal classes, describing its first successful application to coccolithophorids and diatoms. This approach allows us to detect and estimate the size of the C_i pool in cultures at natural cell densities and in an identical water or media chemistry to which cells have been acclimated. Because no specialized equipment beyond that used for standard photosynthetic ^{14}C uptake measurements (incubation of labeled medium, filtration system and scintillation counter) is required, the method might be especially suited for assaying the C_i pool of cells at an array of conditions or in shipboard measurement programs. Complementary experiments, using the ^{14}C disequilibrium method (Elzenga et al. 2000, Espie and Colman 1986, Rost et al. 2007), were used to describe the relationship between active HCO_3^- uptake and the existence and size of the C_i pool.

We investigate Ci pools in two algal classes, one a calcifying strain of the coccolithophorid *Emiliania huxleyi* ((Lohmann) W.W.Hay & H.P.Mohler), and the marine diatom *Thalassiosira weissflogii* ((Grunow) G.Fryxell & Hasle). *E. huxleyi* is well known as a cosmopolitan unicellular calcifying alga which is widely distributed with blooms known to

produce a large quantity of organic matter and calcite before sinking to the bottom of the sea. Therefore, *E. huxleyi* plays an important role in the global C cycle, and enhances the biological pump by transporting C from the sea surface to the sediment (Buitenhuis et al. 2001). Previous investigations demonstrated that blooms of *E. huxleyi* serve as a sink for atmospheric CO_2 (Buitenhuis et al. 1996, Buitenhuis et al. 2001). *T. weissflogii* is a coastal nontoxic ubiquitous centric diatom. Evidence has recently emerged of a C_4-like mechanism for photosynthesis operating as a biochemical CCM in some strains of *T. weissflogii* (Granum et al. 2005, Johnston et al. 2001, Morel et al. 2002, Reinfelder et al. 2000, Reinfelder et al. 2004), underscoring the diversity of CCMs used within marine microorganisms.

EXPERIMENTAL METHODS

Setup of the experiment

Monospecific cultures of *T. weissflogii* (CCMP 1010) and *E. huxleyi* (RCC 1216) were maintained as dilute batch cultures in sterile filtered seawater in 1L acid washed and autoclaved Schott glass bottles. The growth medium was enriched with major nutrients (phosphorus, nitrogen, and silicon), trace metals and vitamins according to the K/5 recipe with or without silicon (Keller et al. 1987). Experiments were carried out under a light:dark (LD) cycle of 16:8 at a constant temperature of 18 °C under saturated light growth conditions (150 $\mu mol \cdot m^{-2} \cdot s^{-1}$ photon flux). A homogeneous distribution of the cells was sustained by placing the cultures on a system providing continuous gentle rotation. The carbonate system was regulated by modifying the pH via additions of 0.5 mol L^{-1} freshly prepared NaOH or HCl solutions to attain medium at three pH ranges, 8.5, 7.9 and 7.4. The changes in extracellular $CO_{2(aq)}$ mediated by the addition of acid or alkali do not aim to simulate the exact changes in the ocean C system expected during the next centuries, which will entail both increased DIC as well as lower pH. Nevertheless, for experiments like those in the current study, the type of pH manipulation we describe has been shown to produce comparable results as experiments bubbling cultures with air of variable CO_2 concentrations (Hoppe et al. 2011, Schulz et al. 2009). The pH was checked during the course of the experiments to verify that increases of the pH did not exceed 0.2 pH units. Cells were acclimated to experimental conditions for 6-8 generations, which is in accordance with previous experiment investigating the impact of changes in the carbonate system on physiological parameters (e.g. Trimborn et al. 2008, 2009, Burkhardt et al. 2001).

Cell counts and cell volume calculations

Live cell counts were made using a Fuchs-Rosenthal haemacytometer with 0.2 mm and 1/16 mm^2 ruling. Two subsamples were counted for each experiment during the pulse and chase incubation (further explanation in the following paragraphs). The cell concentrations estimated for *E. huxleyi* were up to 40-fold higher than those for *T. weissflogii* (Table 3). The incubations with ^{14}C were initiated with cell densities in the range of 3,600 and 36,000 cells·mL^{-1} for *T. weissflogii* and between 70,000 and 163,000 cells·mL^{-1} for *E. huxleyi*, as given in Table 3.

The cell size and volume were measured using a "Nikon eclipse T_i" inverted light microscope. The shape, the volume, and surface calculations differ for both algae. *T. weissflogii* has cylindrical and *E. huxleyi* spherical cells (Hillebrand et al. 1999). 100 individual cells were measured for each experiment (Table 3).

Chla measurements

Samples of 100 ml were filtered through Whatman GF/F filters (pore size 0.8 µm) and stored for not longer than 2 weeks at -20°C until further processing. Following Parsons et al. (1984) total chlorophyll *a* (chl *a*) concentration were estimated by extraction for 24 h in 90 % acetone for fluorometric determination (Turner Designs fluorometer) (excitation 450 nm, emission 670 nm). The concentrations were calculated after correction for phaeopigments (Holm-Hansen et al. 1965, UNESCO 1994).

Carbonate system

The pH measurements were obtained with a pH meter (Crison GLP-21), using a combined glass/ reference electrode type SE 100. The electrode was calibrated with technical buffers (DIN 19267) at pH 4.01, 7.00 and 9.21 and readings are precise to 0.01 units. Shortly before starting the experiment the pH of a subsample of the original culture (100 mL of 1 L) was measured. During the incubation the pH value was checked frequently (every 30 min at

least). Only minimal changes occurred within the pulse and chase incubation period (Table 3). Therefore the starting values were used for further calculations. Alkalinity samples were taken from the filtrate (25 mm GF/F Whatman, approximate pore size 0.8 µm), stored and poisoned with 0.5 mL of an $HgCl_2$ solution (35 g L^{-1}) in 150 mL borosilicate flasks at 4 °C. Total alkalinity (TA) was calculated according to Langmuir after quadruplicate potentiometric titration using a Crison TitroMatic 1S (Bradshaw et al. 1981, Brewer et al. 1986). The complete carbonate system was determined from temperature, salinity (36 PSU), pH, TA, phosphate and silicate concentrations (original medium concentrations were applied) using the program CO2sys (Lewis and Wallace 1998). Equilibrium constants of Mehrbach et al. (1973) refitted by Dickson and Millero (1987) were chosen.

The manipulation of the carbonate system parameters and the use of different initial seawater media due to experiments conducted over the time period of one year led to a range of TA between 1,420 and 3,643 µmol kg SW^{-1} for *T. weissflogii* and between 937 and 2,773 µmol kg SW^{-1} for *E. huxleyi* (Table 3). The seawater was sampled at different times during the year in the Bay of Biscay close to the Spanish coast. Variable circulation regimes and phytoplankton growth (e.g. Llope et al. 2007) result in temporal variation of surface water C chemistry. The reduction of the pH by one unit resulted in a more than 10-fold increase in $CO_{2(aq)}$ concentration (Table 3).

^{14}C pulse-chase incubation – measurements of the C_i pool

The set-up of the experiments followed that described by Berman-Frank and Erez (1996). A rough scheme, presented in Fig. 1 explains the major principles. In general, triplicate culture experiments were done for each setting and species (in total 18 experiments). 250 mL of the cultured populations were spiked with $NaH^{14}CO_3$ (~ 1.7 to 6.4 x 10^4 Bq per 5 mL of cell suspension). The acid-stable photosynthetic uptake of ^{14}C was followed by filtering 5 mL aliquots on 25 mm GF/F Whatman filters, washed thoroughly 5 times with K/5

medium (Keller et al. 1987). Three filters were sampled at each time point during the pulse period. Subsequently, the filters were acidified over concentrated HCl fumes to eliminate residual inorganic ^{14}C as well as unfixed (not incorporated) inorganic ^{14}C inside the cell. Following this, 5 mL scintillation cocktail (Packard, Ultima Gold AB, using the solvent di-isopropylnaphthalene (DIPN),) was added to the vials and the ^{14}C was measured by standard liquid scintillation procedures on a Wallac 1409 Liquid Scintillation Counter. To evaluate the potential for retention of ^{14}C on the surface of cells but which was neither fixed nor part of intracellular C_i pool, individual blanks (time zero – TZ) were performed as follows: after adding the ^{14}C spike to a small subsample of the original culture 4 times 5 ml were filtered immediately. The obtained value reflects the residual inorganic ^{14}C, which was not removed by acidification. The obtained average value was subtracted from all samples (Table 1).

To record the C_i pool, the remaining culture from the pulse incubation was concentrated and washed with non-labeled medium (~150 mL) on a 47 mm 3 µm polycarbonate filter (Millipore), using gentle vacuum. Washing with non-labeled medium assured the removal of cell surface-attached ^{14}C tracer and remaining pulse medium. The washing procedure took less than 5 min and the cells were kept in suspension and were never allowed to dry over the filter in order to minimize any negative impacts by the washing procedure on physiological parameters. Finally, the cells were resuspended in ~150 mL of nonradioactive K/5 medium; silicate was added for the experiments with *T. weissflogii,* and reincubated at the same conditions as before. Cell counts conducted during the chase period confirmed that the washing routine did not damage cells, because cells counts remained the same within counting error as during the pulse period. Sampling, during this chase period, was conducted as described for the pulse period. The ^{14}C levels in the medium were measured during the chase incubation to test for washing efficiency. For that propose, the medium was passed through a 0.2 µm Nuclepore filter and the filtrate was used to assay that the ^{14}C levels were negligible during the chase (chase activity – CA), confirming that no further cellular

uptake of ^{14}C labeled DIC could occur during the chase incubation (Table 1).. In addition, for 12 of the 18 experiments, the CA was measured 5 times during the chase. These measurements revealed no increase of CA in the media during the chase, indicating no detectable leakage of labeled compounds from the cells. To further confirm that no cells were lost during the washing procedure, we determined the remaining labeled material on the washing filter (chase filter – CF). Consistent with data from cell counts, the proportion of the activity measured from the CF confirmed an insignificant decrease/loss of cells during the washing procedure (Table 1). Finally, in filters without cells we verified negligible retention of ^{14}C label on filters following washing.

In parallel, dark incubations were done for four experiments. These were used to ensure that the measured ^{14}C incorporation during the main pulse chase incubations arose from the light dependent photosynthetic uptake. Therefore, a 60 ml subsample of the original culture was spiked and kept in the dark. The samplings proceeded after 5, 30 and 60 min of incubation. The results showed a dark incorporation of less than 3 % compared to the light incorporation (Table 2).

The acid-stable incorporated ^{14}C was used to calculate the photosynthetic C uptake per cell. The amounts of DIC, added activity (AA), blank values as well as the particular cell concentrations were included to estimate the cell-specific photosynthetic C uptake rate according to the following formula:

$$\text{DIC uptake rate}\left[\text{pmol DIC cell}^{-1}\right] = \frac{\text{measured activity}\left[\text{CPM ml}^{-1}\,\text{h}^{-1}\right] - \text{TZ}\left[\text{CPM ml}^{-1}\,\text{h}^{-1}\right]}{\text{cell concentration}\left[\text{ml}^{-1}\right]} \times \frac{\text{DIC}\left[\text{pmol ml}^{-1}\right]}{\text{AA}\left[\text{CPM ml}^{-1}\,\text{h}^{-1}\right]}$$

The efficiency of the AA and the analyzed samples was equal and constant. Hence there was no need to apply quench correction or to include the efficiency in the equation.

An increase of ^{14}C activity during the chase period inside the acid stable fraction was measured for the pH settings ~ 8.5 and ~ 7.9 in the cultures of *E. huxleyi* and *T. weissflogii*.

This increase was interpreted to represent acid stable photosynthetic organic matter that was transferred from the acid-labile C_i pool.

Due to the negligible ^{14}C activity in the incubation medium during the chase (Table 1) the increase of ^{14}C activity in the acid-stable photosynthetic organic matter during the chase must originate from the originally acid-labile intracellular C_i pool. Thus, the C_i pool size per cell is calculated from the difference in photosynthetically fixed acid stable C between the last measurement of the pulse and the maximum value during the chase incubation. This calculation reflects only a minimum estimate of the C_i pool because the sampling was not continuous and therefore the maximum peak during the chase might have been missed. Though our tests suggest only a minor loss of label from cells, the washing procedure may have also caused some leakage of ^{14}C from the cells, and some ^{14}C may be lost due to respiration and secretion of dissolved organic C. In converting the absolute C_i pool to an estimated concentration in the cell, we use cell numbers and the total cellular volume. While the $CO_{2(aq)}$ accumulation in eukaryotic algae is considered to be restricted to the chloroplast or even the pyrenoid (Badger et al. 1998), the total degree of intracellular DIC enrichment is calculated as if the full cell volume (e.g. cytoplasm) hosted the C_i pool. In part, this convention is adopted because the volume of the entire cell is much more tightly constrained than the volume of intracellular compartments(Badger and Lorimer 1976, Kaplan et al. 1980). This approach of not accounting for the possible localization of C_i in specific cellular compartments might result underestimating the relative enhancement at the site of RubisCO compared to concentration in the incubation medium.

We infer an operationally-defined C_i pool, which is the acid-labile C within the cell which is subsequently available as a substrate for photosynthesis. The approach does not distinguish the form in which the C is stored within the cell, which could be as DIC or as an acid-labile organic complex. However, in whatever form the C is present, it is subsequently available for conversion to CO_2, the only substrate used by RubisCO during photosynthesis.

^{14}C disequilibrium method

The theory and methodology of this technique has been described extensively in several articles (e.g. Elzenga et al. 2000, Martin and Tortell 2006). The method is based on the slow interconversion between HCO_3^- and CO_2, which allows differential labeling of the DIC species with ^{14}C over several minutes. In the Hepes buffered DIC spike solution (pH 7.0) $^{14}CO_2$ represents 20% of the total C_i pool. On the other hand, CO_2 accounts for only 0.4 % of the total DIC in the Bicine buffered medium (pH 8.5) of the cell suspension. Therefore initially the specific activity (dpm mol^{-1}) of CO_2 in the spike solution is high and it decays exponentially to an equilibrium value over the duration of the assay. Phytoplankton species which base their growth on CO_2 exclusively reflect these changes unaltered. In contrast, species relying predominantly on HCO_3^- show a near constant ^{14}C incorporation rate, resulting in a linear plot. The uptake curves are best modeled according to models calculated by Elzenga et al. (2000) and Rost et al. (2007).

$$\mathrm{DPM_t} = \mathrm{V_t}(1-f)(\alpha_1 \mathrm{t} + (\Delta \mathrm{SA_{CO2}} / \mathrm{SA_{DIC}})(1-e^{-\alpha 1 t})) / \alpha_1 + \mathrm{V_t}(f)(\alpha_2 \mathrm{t} + (\Delta \mathrm{SA_{HCO3}} / \mathrm{SA_{DIC}})(1-\mathrm{e}^{-\alpha 2 \mathrm{t}}))/\alpha_2 \quad (303)$$

V_t is the total rate of DIC uptake; f is the fraction of uptake attributable to HCO_3-; α_1 and α_2 are the temperature-, salinity-, and pH dependent first order rate constants for CO_2 and HCO_3^- hydration and dehydration (Espie and Colman 1986). Under the experimental conditions (18°C, salinity 36, pH 8.5) α_1 and α_2 are 0.0383 and 0.0456 s^{-1}, respectively. ΔSA_{CO2} and ΔSA_{HCO3} are the differences between the initial and equilibrium values of the

specific activity of CO_2 and HCO_3^-, and SA_{DIC} is the specific activity of all inorganic C species at equilibrium. The values of $\Delta SA_{CO2}/SA_{DIC}$ and $\Delta SA_{HCO3}/SA_{DIC}$ are set by the difference in pH between the ^{14}C spike and seawater buffer. The values used during our experiments were 49 and -0.19 for $\Delta SA_{CO2}/SA_{DIC}$ and $\Delta SA_{HCO3}/SA_{DIC}$, respectively.

The ^{14}C disequilibrium method largely followed the experimental protocol described by Rost et al. (2007, 2006). First of all the culture was concentrated (roughly 20 fold, determined by measuring the chl*a* content of the original culture and concentrated suspension, data not shown). During this process the original medium was exchanged with a BICINE buffered medium (BICINE 20 mmol L^{-1}, pH 8.5). A 4 mL aliquot was directly transferred into a glass cuvette placed on a stirrer to maintain uniform distribution of the cells. Light and temperature were kept constant using an additional light source (150·µmol·m^{-2}·s^{-1} photon flux) and connecting a water chiller to the glass cuvette. After a pre-incubation of about 10 min a 10 µCi ^{14}C spike of pH 7.0 (HEPES 50 mmol L^{-1}) was injected. Afterwards, subsamples of 200 µL were withdrawn at short time intervals and dispensed into 2.0 mL of HCl (6 mmol·L^{-1}) to stop C incorporation. The residual ^{14}C was removed by putting the subsamples for 8h on a shaker. Subsequently, 10 mL of the scintillation cocktail (Packard, Ultima Gold AB) was added and ^{14}C was measured, using standard liquid scintillation procedures. Blanks, spike added to cell free buffers, were subtracted from all samples. To examine the CO_2 : HCO_3^- ratios taking into account the impact of eCA, the ^{14}C disequilibrium method was run in two ways; one control run and one run where we added the membrane-impermeable inhibitor dextran-bound sulfonamide (DBS, Synthelec AB). The inhibitor was added to a final concentration of 50 µmol L^{-1} at least 10 min prior to the experiments. DBS is known to inhibit eCA effectively. This was proven by Moroney et al. (1985) using bovine carbonic anhydrase in a potentiometric assay. This inhibitor exhibits similar activities to AZ (Elzenga et al. 2000).

RESULTS

Table 3 summarizes the carbonate system chemistry for the experiments. The experiments were conducted in February 2011 and December 2011, therefore different seawater was used during the incubations, and this caused some variations in the carbonate system. In all cases, the three pH levels clearly induced different $CO_{2(aq)}$ concentrations : pH ~ 8.5: 1 to 9 µmol kg SW^{-1}; pH ~ 7.9: 16 to 32 µmol kg SW^{-1}; pH ~ 7.4: 34 to 85 µmol kg SW^{-1} (Table 3).

In general, cell concentrations of *T. weissflogii* and *E. huxleyi* differed among the species and the single experiments (Table 3). Experiments of *E. huxleyi* typically contained 10 times higher cell concentrations than those of *T. weissflogii*. The cell volume of *T. weissflogii* varied between 960 µm^3 and 2098 µm^3 (Table 3). Significant correlations between cell volume and the applied pH settings could not be retrieved. The cell volume of *E. huxleyi* varied between 17.6 and 37.7 µm^3 (Table 3), with larger cells at lower pH values.

Pulse chase method

Because the pulse chase method was previously employed in only one other phytoplankton species (Berman-Frank and Erez 1996), we conducted several tests to examine the viability of this approach (Table 1). TZ samples acting as blanks were low, always less than 1 ‰ of the AA and never more than 5 % of the maximum uptake during the pulse period. Also the CA was small compared to the AA (< 1%) and no increase of the CA was detected during the chase. This and the negligible loss of cells (e.g. retained on the CF), demonstrated an effective washing without adverse effects on the cell population. In addition, we measured the dark C fixation (Table 2). Dark fixation rates in the acid stable particulate organic matter of *T. weissflogii* and *E. huxleyi* never exceeded 2.5 % of the light fixation. These values

confirm that photosynthetic fixation by RubisCO is the main mechanism for C incorporation into cellular material, with negligible surface absorption of label.

The pH affected the gross ^{14}C incorporation rates, measured during the pulse period of *E. huxleyi* (Fig. 2, Table 3), with highest uptake rates at the pH level of ~ 7.9. We found reduced rates at higher and lower pH values, indicating better growth conditions at the intermediate pH. No clear trend in ^{14}C incorporation rate with pH is evident in the diatom *T. weissflogii*, due to the high variability in incorporation rates in different replicate experiments. The fixation rates per cell are several orders of magnitude higher for *T. weissflogii* than for *E. huxleyi*, likely due to the much larger cell size and C demand of *T. weissflogii*.

During the chase period, the fixed ^{14}C per cell continued to increase for both species in all but the lowest pH condition ~7.4 (Fig. 3, 4). This implies a transfer of ^{14}C from the acid labile reservoir to the acid stable matter inside the cell. The increase had to arise from an acid-labile C_i pool, labeled with ^{14}C during the pulse, because no further ^{14}C supply occurred from the medium during the chase incubation. The degree of increase in fixed ^{14}C per cell, relative to the total uptake of ^{14}C during the pulse, defined the fraction of fixation supported by the C_i pool, which varied according to the extracellular pH/ $CO_{2(aq)}$ concentration (Table 3, Fig. 5). *T. weissflogii* showed a significant pool at high (0.5 – 2.1 nmol·cell^{-1}) and intermediate (0.5 – 1.4 nmol·cell^{-1}) pH values (low and intermediate $CO_{2(aq)}$ levels (Fig. 5a, b)), and a negligible C_i pool at low pH or high $CO_{2(aq)}$. Beyond that, a positive correlation between the DIC concentration in the extracellular medium and the size of C_i pool of *T. weissflogii* was detected (Fig. 5c). *E. huxleyi* showed a significant C_i pool at high and intermediate pH levels, respectively low or intermediate $CO_{2(aq)}$ concentrations, too (Table 3). However, in *E. huxleyi*, there is no significant correlation between the extracellular DIC concentrations and the pool size (Fig. 5f). Only at the lowest $CO_{2(aq)}$ or highest pH of 8.5 (Figure 5d) did the *E. huxleyi* exhibit higher C pool size for high C_i media compared to lowest C_i. This trend is also

evident at both intermediate and high pH levels, for *T. weissflogii.* Overall, the cell-specific absolute C_i pool size of *T. weissflogii* was up to 230 fold higher than the one for *E. huxleyi* (Table 3, Fig. 5), consistent with the differences of total photosynthetic rate per cell and cell volume mentioned earlier. In contrast to previous investigations, the enhancement of intracellular acid-labile C pool vs. extracellular DIC was calculated based on culture media with natural seawater DIC concentrations in the culture medium rather than synthetic low DIC media. The enhancement for *T. weissflogii* varied at pH ~ 8.5 between 2.5 and 14.3, at pH ~ 7.9 between 1.1 and 4.4 and almost no enhancement was detected at pH ~ 7.4. *E. huxleyi* showed also three distinct levels of C_i accumulation inside the cell. We calculated following ratios: pH ~ 8.5 1.1 to 2.1 fold elevation, pH ~ 7.9 0.2 to 0.5-fold elevation, at pH ~ 7.4 no accumulation.

In both species, the cellular *Chla* was reduced at the lowest pH, at which $CO_{2\ aq}$ was highest (Fig. 6). As soon as a C_i pool in *T. weissflogii* cells was measured, the Chl*a* content increased (Fig. 6b). Nonetheless the Chl*a* content of *E. huxleyi* seemed to be related differently to the C_i pool. Maximum C_i pool values coincided with intermediate Chl*a* values, and no linear relationship between Chl*a* concentrations and the C_i pool, was detected in this species (Fig. 6e). Normalizing the Chl*a* content per cell to the cell volume does not significantly modify trends for either *T. weissflogii* or *E. huxleyi* (Fig. 6c, f).

^{14}C disequilibrium method

In addition, we applied the ^{14}C disequilibrium method to reveal one part of the CCMs, active HCO_3^- uptake vs. passive or active CO_2 uptake used for photosynthesis. *E. huxleyi* showed decreasing HCO_3^- uptake at high CO_2 levels (low pH values) (Fig. 7c, d, e, 8). The acid-stable C_i uptake was dominated by HCO_3^- (60 %) at a pH of 8.11, while at a pH of 7.49 when no pool was detected, the photosynthetic C demand was mainly satisfied by CO_2 (61.2 % CO_2, 38.8 % HCO_3^-). Investigations using the ^{14}C disequilibrium method on *T. weissflogii*

indicated similar proportion of HCO_3^- and CO_2 incorporation at a pH of ~7.5 and 7.9. In both conditions, the C_i uptake was dominated by CO_2 (60 %) while HCO_3^- contributed 40 % of C to photosynthesis (Fig. 7a, b, 8). In both the diatom and coccolithophorid, HCO_3^- uptake, though not dominant, was still a significant source of C fixed by photosynthesis at the lowest pH, respectively highest $CO_{2(aq)}$ levels, even though no intracellular C enrichment could be measured (Table 3, Fig. 5).

DISCUSSION

Application of the pulse-chase method

The evaluation of CCMs and related changes of the intracellular C system of different phytoplankton species provide important information concerning species competition and success. Therefore, several approaches and methods were invented to detect and analyze the C_i pool during the past 30 years (e.g. Badger et al. 1980, Badger et al. 1985, ter Kuile and Erez 1987). To date, none have been extensively applied to evaluate response of CCMs over a range of naturally occurring C conditions. Our results, using the pulse chase method, give C_i accumulations which are comparable to those obtained by the silicone oil centrifugation method (SOC) or to measurements of mass spectrometry analysis (MIMS) (Table 4) (Badger et al. 1980, Badger et al. 1985, Kaplan et al. 1980).

The pulse chase method provides several advantages compared to SOC or MIMS. Unlike SOC or MIMS, the pulse chase method is employed at ambient DIC concentrations. We used extracellular DIC concentrations similar to the natural DIC concentrations in the ocean (approximately 2000 µmol L^{-1},(e.g. Takahashi et al. 2002)), contrasting to most previous studies of C concentration factors inside the cell obtained with SOC or MIMS, conducted at much lower DIC concentrations of 100 to 1000 µmol L^{-1} in the incubation medium (Table 4). For SOC and MIMS analysis generally, the cells have to be transferred to DIC depleted medium (e.g. Badger et al. 1980, Badger et al. 1985, Rost et al. 2007). Such large changes were reported to reduce the intracellular pH about 0.7 (~ 7 to 6.3) within 35 to 40 min (Nimer et al. 1994). Recent investigations also shown that large increments of HCO_3^- (concentrations up to 20 mmol L^{-1}), result in lowering the intracellular pH of *E. huxleyi* within seconds (Suffrian et al. 2011). This causes changes of pH within the cell and alters the C speciation in the cytosol. Therefore, it is possible that even short time incubations at DIC depleted conditions affect the size and the measurements of C_i pools of unicellular algae, due

to enhanced or reduced diffusion of CO_2 between cell compartments or the cell and the surrounding medium.

The pulse chase method investigates C_i pools at the original culture cell density. We used the same cell concentrations as achieved at the end of the acclimation to the particular pH setting. In contrast, cell concentrations used for SOC and MIMS have to be strongly increased to obtain measurable signals even during short incubations (e.g. Dong et al. 1993, Nimer et al. 1994, Nimer et al. 1992, Tortell et al. 2000, Woodger et al. 2003). The short incubation time, 10 s for the SOC and 10 min for the MIMS analysis, again is caused by the DIC depleted medium used therein. Longer incubation would hamper photosynthesis and alter the analysis at these strongly modified conditions, whereas the pulse chase incubations proceded at DIC replete conditions and the incubation period last at least for 2 hours. Prolonging the incubation time increased the sensitivity and even lower cell concentrations still showed sufficient radioactive signals, when using the pulse chase method. *In situ* studies reported similar cell densities to those presented here for *E. huxleyi* (Berge 1962), while *in situ* concentrations for *T. weissflogii* are probably somewhat lower than the ones used here.

Furthermore, the pulse chase method uses infrastructure which is already standard for routine measurements of primary production via ^{14}C uptake, and therefore might be an optimal choice during seagoing field campaigns.

Certainly, it is also required to discuss the drawbacks of the pulse chase method. It provides a smaller array of data than MIMS or SOC analysis, where e.g. it is possible to measure the photosynthetic oxygen evolution or half saturation constants of photosynthetic DIC uptake (e.g. Badger et al. 1985, Nimer et al. 1992, Spijkerman 2011). Beyond that, the C_i pool detection with SOC or MIMS can quantify changes inside the pool in less than 2 min., shown for *Synechococcus* sp or *Anabaena variabilis* (Kaplan et al. 1980, Miller et al. 1988), whereas, the pulse-chase C_i pool method can only be applied to species or phytoplankton

samples with relatively long pool turnover times (e.g. of order 10 minutes or longer). This stems from the non-continuous measurements via the filtration procedure (roughly every 5 min), and the conservative assumption that a one point measurement is not sufficient, resulting in a typical 10 minute interval for calculating the C_i pool during the chase. Therefore, this method is suitable for eukaryotic phytoplankton or large prokaryotic ones. The detection limit depends on the DIC incorporation rate but higher DIC incorporation rates are usually associated with faster intracellular C_i turnover rates. Turnover times are expected to be inversely proportional to cell surface area:volume , and therefore may be very fast for small cyanobacteria but much longer for the coccolithophorids or diatoms in this study whose surface area:volume ratios (Table 3) are nearly an order of magnitude larger than those reported for cyanobacteria (Popp et al., 1998). The absence of detectable ^{14}C label in the chase media in our coccolithophorid and diatom experiments is also consistent with a slow turnover of the C_i pool.

In all cases, the pulse chase evaluations reflect a minimum estimate for the C_i pool. First of all because measurements were made every 5 min, and the maximum peak of ^{14}C incorporation during the chase period might have occurred in between sampling. In addition, though of minor importance, some ^{14}C may be lost due to leakage of any labeled CO_2, as well as respiration and secretion of dissolved organic C. The estimate of the CCF is also likely to reflect a minimum estimate in all methods, because the C_i pool probably is restricted to one compartment of the cell, the chloroplast or pyrenoid, rather than the entire cell volume, as described in detail in the subsequent section.

Evaluating calculated CCF

The CCF is an indicator of the average enrichment of C in the cell because it considers the entire cell volume as hosting the C_i pool. In reality the C_i pool may be hosted in a much smaller volume at the site of RubisCO and therefore provide a much greater actual enrichment

of CO_2 to RubisCO. Traditionally, the CCF has been calculated by using the ratio of C_i pool vs. extracellular DIC concentration (Badger et al. 1985, Kaplan et al. 1980, Spijkerman 2011). Because our natural seawater DIC concentrations were higher than many previous experiments, our CCFs are at the lower end or below those obtained in previous studies (Table 4), even though the absolute acid-labile C_i pool concentrations are much higher. *E. huxleyi*, for example, shows CCFs less than 1 at a pH of 7.9, nonetheless a C_i pool exists (Fig. 3). We propose, that the calculated intracellular acid-labile C concentrations up to 928 µmol L^{-1}, though lower than the extracellular DIC concentration, cannot be maintained by passive C uptake, via $CO_{2(aq)}$ diffusion only. Published estimates on the CCF for the diatom *T. weissflogii* are lacking, although other diatoms, e.g. *Phaeodactylum tricornutum* are also known to increase intracellular DIC concentrations at low $CO_{2(aq)}$ concentrations (Badger et al. 1998, Colman and Rotatore 1995).

C_i pool

We showed a pH or $CO_{2(aq)}$ dependent C_i pool for *T. weissflogii* and *E. huxleyi,* with higher intracellular DIC concentrations at high pH levels corresponding to low $CO_{2(aq)}$ concentrations (Figure 5 a, b, d, e). The presence of a C_i pool in *E. huxleyi* and *T. weissflogii* at high pH or low $CO_{2(aq)}$ indicates that CCMs are active in both species, consistent with a broad array of CCM measurements (e.g. Burkhardt et al. 2001, Rost et al. 2003) CCMs evolved in relation to inorganic C limitation of photosynthesis (e.g. Giordano et al. 2005). Nevertheless, a C_i pool alone does not encourage photosynthesis: an additional mechanism (e.g. iCA, thylakoid CA) that converts the stored C at a rate sufficient to saturate the demand of RubisCO is required (e.g. Raven 1997). Besides the positive correlation between pH and the size of the C_i pool, and the negative correlation between $CO_{2(aq)}$ concentration and the size of the C_i pool for both species, we also found a significant relation between extracellular DIC concentrations and the C_i pool for *T. weissflogii* (Fig. 5c) at intermediate and highest pH

conditions. This suggests the potential for bicarbonate regulation of the CCM in diatoms and merits further investigation. One mechanism might be that higher DIC facilitates greater HCO_3^- uptake which is especially significant if *T. weissflogii* employs a C_4 mechanism as part of its CCM (McGinn and Morel 2008, Reinfelder 2011, Reinfelder et al. 2000). In *E. huxleyi*, there is no clear evidence for a strong correlation between extracellular DIC concentration and the size of the pool (Fig. 5f).

The C_i pool concentrations (Table 4) are higher than the range of previous values identified for *E. huxleyi* and many other marine phytoplankton species, using the SOC or MIMS approach, probably caused by our higher DIC concentrations in the culture medium (Table 3, 4). This observation suggests that higher DIC values increase the absolute C_i pool. In addition, it might be possible that in contrast to the SOC and MIMS experiments, the longer incubation period with ^{14}C in the pulse-chase approach permitted some fraction of cellular DIC uptake to be bound to organic compounds within the cell rather than remaining as free CO_2, HCO_3^-, or CO_3^{-2}. Because any intracellular C eventually reconverted to CO_2 for photosynthesis is detected by the pulse-chase approach, the pulse-chase method may detect this broader array of acid-labile C_i components. In contrast, SOC and MIMS measurements may detect only the free CO_2, HCO_3^-, or CO_3^{-2}.

Due to totally different media compositions between MIMS and SOC and the pulse chase method, the results of *E. huxleyi* cannot be directly compared with previous results summarized in Badger et al. (1998). Comparing our measurements of the enrichment inside the cell for *E. huxleyi* and *T. weissflogii*, it is obvious that the diatom exhibits greater elevation than the coccolithophorid (Table 3, 4). We assume that more effective CCMs result in higher intracellular DIC concentrations in diatoms.

Previous investigations showed that diatoms evolved later than coccolithophorids and therefore might be adapted to lower atmospheric CO_2 levels (Tortell 2000). It was supposed

that diatoms develop higher RubisCO specificity factors than coccolithophorids and therefore might not need a great C_i pool (Tortell 2000). Nonetheless, our data for the diatom *T. weissflogii* indicate that the CCMs employed by diatoms may also require C_i pools.

We identified an important threshold of 30 µmol·L^{-1} $CO_{2(aq)}$ for the establishment of a detectable C_i pool in both *E. huxleyi* and *T. weissflogii*. The threshold for *Peridinium gatunense* was 15 µmol L^{-1} (Berman-Frank and Erez 1996). To date, thresholds for C_i pool development have not been widely investigated. Our new data are among very few reported estimates of threshold for C_i pool of phytoplankton species.

CO_2 vs. HCO_3^- uptake

Information available on the proportion of CO_2 or HCO_3^- used for photosynthesis has been provided by the ^{14}C disequilibrium method and MIMS. These techniques have been used to assess changes in substrate as a function of environmental conditions both in cultures and natural populations. The intercomparison of both methods shows consistent results (Rost et al. 2007). More recently both methods have also been in oceanographic field studies, demonstrating that HCO_3^- is the major source of DIC to satisfy the demand of photosynthesis (Martin and Tortell 2006, Tortell et al. 2006).

E. huxleyi is known to exhibit large strain-specific physiological responses (e.g. Hoppe et al. 2011, Langer et al. 2009). The strain of *E. huxleyi* used in our experiments appears to satisfy about 50 % of the photosynthetic DIC demand by HCO_3^- when grown under present atmospheric conditions (Morel et al. 2002, Rost et al. 2007). Some other strains exhibit a lower proportion of HCO_3^- to satisfy the photosynthetic DIC demand at present day CO_2 concentrations (Fig. 8; data from Rost et al (2003)). Nevertheless, different *E. huxleyi* strains showed similar trends of increased reliance on CO_2 for photosynthesis as CO_2 availability increased. Focusing on our ^{14}C disequilibrium results, we observed even though no acid-labile

C_i pool was detected for *E. huxleyi* at a pH of 7.49, nearly 40 % of the photosynthetic DIC demand was covered by HCO_3^-. That indicates that active transport of HCO_3^- still supplies photosynthesis without appreciable intracellular accumulation. Such a mechanism has been described previously by Raven (1997), who suggested that autotrophic cells rely on an acidified thylakoid lumen and a high thylakoid CA activity, and suggested that this CA is a dominant element of the CCM in this pH range.

T. weissflogii is known to satisfy the photosynthetic DIC demand with approximately 70 % in the form of HCO_3^- at present $CO_{2(aq)}$ concentrations (Burkhardt et al. 2001, Morel et al. 2002) (Fig. 6). The DIC acquisition of *T. weissflogii* follows the HCO_3^- user model, in detail explained by Trimborn et al. (2008). Again, HCO_3^- is not the dominant source at lowest pH 7.49, but high proportions of HCO_3^- incorporation relative to total photosynthetic DIC incorporation imply an active transport of HCO_3^-, supplying photosynthesis without appreciable intracellular accumulation.

Photosynthetic DIC incorporation rates – Chla content

Much effort has been invested in characterizing the response of algal growth rate to increasing $CO_{2(aq)}$, to assess whether reduced reliance on CCMs permits reallocation of resources to enhance growth. The DIC incorporation rates measured during the pulse (120 min) may not be representative of average steady state growth rates integrated over several days (Hurd et al. 2009). The enormous difference of 1000 in magnitude for the DIC incorporation rates for *T. weissflogii* and *E. huxleyi* (Table 3), might be due to a reduced light level during the pulse chase experiments, compared to the light levels needed for optimal growth of *E. huxleyi* (Oguz and Merico 2006). Other possibilities are higher leakage of DIC by *T. weissflogii* or release of fixed DIC as DOC, this phenomenon of wasting high energy-demanding products was also reported for diazotrophic cyanobacteria with respect to N_2 fixation and DON (Ohlendieck et al. 2000, Wannicke et al. 2009). However, during our brief

incubation *T. weissflogii* and *E. huxleyi* both exhibited highest DIC incorporation rates at a pH of ~7.9 (Fig.2). This emphasizes that both species are well adapted to the present state $CO_{2(aq)}$, concentrations or rather what is expected for the end of this century. Lower and higher pH values resulted in clearly reduced DIC incorporation rates. Previous studies examined growth for *E. huxleyi* in the pH range of 7.7 and 8.6, a range in which some strains exhibit decreasing growth at pH below 7.8, others including the strain used here exhibit constant growth, and some show increasing autotrophic growth (Feng et al. 2008, Hoppe et al. 2011, Iglesias-Rodriguez et al. 2008, Langer et al. 2009, Riebesell et al. 2000). It is possible that suboptimal growth conditions, caused by the more extreme acidic conditions at the pH of 7.45, negatively affected the DIC incorporation rate. Photosynthesis of *T. weissflogii* was previously shown to be positively influenced by enhanced CO_2 concentrations (Burkhardt et al. 2001). We found the proposed stimulation just between the highest and medium pH level. In accordance to those findings, *E. huxleyi* and *T. weissflogii* had the highest Chl*a* cell contents at a pH of ~7.9 (Fig. 6). Furthermore, it has to be kept in mind that the amount of RubisCO per Chl*a* might be influenced by different $CO_{2(aq)}$ concentrations (Yokota and Canvin 1985). Increasing the chlorophyll content of the cell has been described as one potential adaptation to stress (Geider, 1987, Riemann et al., 1989). Even though no linear relationship between the Chl*a* content and $CO_{2(aq)}$ concentrations was detected, the RubisCO content and therefore also the efficiency might also have varied. Suboptimal growth conditions at the pH level of ~7.4 were indicated by clearly reduced Chl*a* contents (Fig. 6).

Conclusions

The pulse-chase C_i pool detection method, extended here to coccolithophorids and diatoms, provides an effective and routine method for characterizing the acid-labile C pool that is applicable to all the main classes of marine eukaryotic plankton. Our results confirm that both a diatom and a calcifying coccolithophorid build significant intracellular C_i pools

over the lower range of CO_2 investigated here (~ 2 to 30 µmol·L^{-1} $CO_{2(aq)}$, respectively pH 8.6 - 7.91). These CO_2 values encompass the range found in most modern surface seawaters, for example from cold upwelling areas to warm subtropical gyres (Borges et al. 2005, Laws et al. 1997, Takahashi et al. 2002). Therefore a great benefit of the application of the ^{14}C-pulse chase method is its feasibility at natural seawater DIC concentrations, so that results may be compared with natural populations.

For both algal classes, the C_i pool becomes a negligible contributor to photosynthesis once $CO_{2(aq)}$ exceeds 30 µmol·L^{-1}. Thus, in the range of surface waters conditions predicted for the year 2100 (Houghton et al. 2001) especially in the most CO_2-rich areas of the ocean, this aspect of CCMs may be of reduced importance.

Diatoms and coccolithophorids are both key taxa to the effective operation of the biological C pump and the ratio of the export production of these groups sets the deep ocean alkalinity and ocean/atmosphere CO_2 partitioning (Laws et al. 1997, Laws et al. 2002). If our method can be used to assess whether the main exported species of coccolithophorids and diatoms will have different or similar thresholds for foregoing significant acid-labile intracellular C accumulation for photosynthesis , we could better predict the response of marine biogeochemical cycling to anthropogenic C cycle changes.

ACKNOWLEDGEMENTS AND AUTHOR CONTRIBUTINOS

We thank Björn Rost and Scarlett Trimborn for introducing us to the ^{14}C disequilibrium method. The work was funded by the European Union under ERC240222-PACE (to HMS). K.I. and J.E. conducted experiments, K.I. and H.M.S. wrote the paper with input from J.E.

REFERENCES

Aizawa K, Miyachi S (1986) Carbonic anhydrase and CO_2 concentrating mechanisms in microalgae and cyanobacteria. FEMS Microbiol Lett 39: 215-233

Badger MR, Andrews TJ, Canvin DT, Lorimer GH (1980) Interactions of hydrogen peroxide with ribulose bisphosphate carboxylase oxygenase. J Biol Chem 255: 7870-7875

Badger MR, Andrews TJ, Whitney SM, Ludwig M, Yellowlees DC, Leggat W, Price GD (1998) The diversity and coevolution of RubisCO, plastids, pyrenoids, and chloroplast-based CO_2-concentrating mechanisms in algae. Can J Bot 76: 1052-1071

Badger MR, Bassett M, Comins HN (1985) A Model for HCO_3 accumulation and photosynthesis in the cyanobacterium *Synechococcus* sp: Theoretical predictions and experimental observations. Plant Physiol 77: 465

Badger MR, Lorimer GH (1976) Activation of ribulose 1,5 bisphosphate oxygenase. The role of Mg^{2+}, CO_2, and pH. Arch Biochem Biophys 175: 723-729

Berge G (1962) Discoloration of the sea due to *Coccolithus huxleyi* 'bloom'. Sarsia 6: 27-40

Berman-Frank I, Erez J (1996) Inorganic carbon pools in the bloom-forming dinoflagellate Peridinium gatunense. Limnology and Oceanography 41: 1780-1789

Berman-Frank I, Zohary T, Erez J, Dubinsky Z (1994) CO_2 availability, carbonic anhydrase, and the annual dinoflagellate bloom in Lake Kinneret. Limnol Oceanogr 39: 1822-1834

Borges AV, Delille B, Frankignoulle M (2005) Budgeting sinks and sources of CO_2 in the coastal ocean: Diversity of ecosystems counts. Geophys Res Lett 32: L14601, doi:10.1029/2005GL023053

Bradshaw AL, Brewer PG, Shafer DK, Williams RT (1981) Measurements of total carbon dioxide and alkalinity by potentiometric titration in the GEOSECS program. Earth and Planet Sc Lett 55: 99-115

Brewer PG, Bradshaw AL, Williams RT (1986) Measurements of total carbon dioxide and alkalinity in the North Atlantic Ocean in 1981. In: Trabalka JR, Reichle DE (eds) The changing carbon cycle: A global analysis, Springer, New York, pp 348-370

Buitenhuis E, Van Bleijswijk J, Bakker D, Veldhuis M (1996) Trends in inorganic and organic carbon in a bloom of *Emiliania huxleyi* in the North Sea. Marin Ecol Progr Ser 143: 271-282

Buitenhuis ET, van der Wal P, de Baar HJW (2001) Blooms of *Emiliana huxleyi* are sinks of atmospheric carbon dioxide: A field and mesocosm study derived simulation. Global Biogeochem Cycles 15: 577-587

Burkhardt S, Amoroso G, Riebesell U, Sültemeyer D (2001) CO_2 and HCO_3^- uptake in marine diatoms acclimated to different CO_2 concentrations. Limnol Oceanogr 46: 1378-1391

Cassar, N., Laws, E.A., & Popp, B.N. (2006), Carbon isotopic fractionation by the marine diatom *Phaeodactylum tricornutum* under nutrient- and light-limited growth conditions. *Geochimica et Cosmochimica Acta* 70, 5323-5335

Colman B, Rotatore C (1995) Photosynthetic inorganic carbon uptake and accumulation in two marine diatoms. Plant, Cell Environ 18: 919-924

Dickson AG, Millero FJ (1987) A comparison of the equilibrium constants for the dissociation of carbonic acid in seawater media. Deep Sea Res Part A 34: 1733-1743

Dong LF, Nimer NA, Okus E, Merrett MJ (1993) Dissolved inorganic carbon utilization in relation to calcite production in *Emiliania huxleyi (*Lohmann) Kamptner. New Phytol 123: 679-684

Elzenga JTM, Prins HBA, Stefels J (2000) The role of extracellular carbonic anhydrase activity in inorganic carbon utilization of *Phaeocystis globosa* (Prymnesiophyceae): A comparison with other marine algae using the isotopic disequilibrium technique. Limnol Oceanogr 45: 372-380

Espie GS, Colman B (1986) Inorganic carbon uptake during photosynthesis: I. A theoretical analysis using the isotopic disequilibrium technique. Plant Physiol 80: 863-869

Feng Y, Warner ME, Zhang Y, Sun J, Fu FX, Rose JM, Hutchins DA (2008) Interactive effects of increased pCO_2, temperature and irradiance on the marine coccolithophore *Emiliania huxleyi* (Prymnesiophyceae). Eur J Phycol 43: 87-98

Geider, R.J., (1987). Light and temperature dependence of the carbon to chlorophyll a ratio in microalgae and cyanobacteria: Implications for physiology and growth of phytoplankton. New Phytol.106, 1 – 34.

Giordano M, Beardall J, Raven JA (2005) CO_2 concentrating mechanisms in algae: mechanisms, environmental modulation, and evolution, Annu Rev Plant Biol 55: 99-131.

Granum E, Raven JA, Leegood RC (2005) How do marine diatoms fix 10 billion tonnes of inorganic carbon per year? Can J Bot 83: 898-908

Hillebrand H, Dürselen CD, Kirschtel D, Pollingher U, Zohary T (1999) Biovolume calculation for pelagic and benthic microalgae. J Phycol 35: 403-424

Holm-Hansen O, Lorenzen CJ, Holmes RW, Strickland JDH (1965) Fluorometric determination of chlorophyll. J Cons Cons Int Explor Mer 39: 3-15.

Hoppe CJM, Langer G, Rost B (2011) *Emiliania huxleyi* shows identical responses to elevated pCO_2 in TA and DIC manipulations. J Exp Mar Biol Ecol 406: 54-62

Houghton JT, Ding Y, Griggs DJ, Noguer M, van der Linden PJ, Dai X, Maskell K, Johnson CA (2001) IPCC, 2001: Climate Change 2001: The Scientific Basis. Contribution of Working Group I to the Third Assessment Report of the Intergovernmental Panel on Climate Change, Cambridge University Press, pp 1-881

Hurd CL, Hepburn CD, Currie KI, Raven JA, Hunter KA (2009) Testing the effects of ocean acidification on algal metabolism: Considerations for experimental designs. J Phycol 45: 1236-1251

Iglesias-Rodriguez M, Halloran PR, Rickaby REM, Hall IR, Colmenero-Hidalgo E, Gittins JR, Green DRH, Tyrrell T, Gibbs SJ, Von Dassow P, Rehm E, Armbrust E, Boessenkool KP (2008) Phytoplankton calcification in a high-CO_2 world. Science 320: 336-340

Johnston AM (1991) The acquisition of inorganic carbon by marine macroalgae. Can J Bot 69: 1123-1132

Johnston AM, Raven JA, Beardall J, Leegood RC (2001) Carbon fixation: Photosynthesis in a marine diatom. Nature 412: 40-41

Kaplan A, Badger MR, Berry JA (1980) Photosynthesis and the intracellular inorganic carbon pool in the bluegreen alga *Anabaena variabilis*: Response to external CO_2 concentration. Planta 149: 219-226

Kaplan A, Reinhold L (1999) CO_2 concentrating mechanisms in photosynthetic microorganisms. Annu Rev Plant Biol 50: 539-570

Keller MD, Selvin RC, Claus W, Guillard RRL (1987) Media for the culture of oceanic ultraphytoplankton. J Phycol 23: 633-638

Langer G, Nehrke G, Probert I, Ly J, Ziveri P (2009) Strain-specific responses of *Emiliania huxleyi* to changing seawater carbonate chemistry. Biogeosciences 6: 2637-2646

Laws EA, Bidigare RR, Popp BN (1997) Effect of growth rate and CO_2 concentration on carbon isotopic fractionation by the marine diatom *Phaeodactylum tricornutum*. Limnol Oceanogr 42: 1552-1560

Laws EA, Popp BN, Cassar N, Tanimoto J (2002) ^{13}C discrimination patterns in oceanic phytoplankton: Likely influence of CO_2 concentrating mechanisms, and implications for palaeoreconstructions. Funct Plant Biol 29: 323-333

Lewis E, Wallace D (1998) Program developed for CO2 system calculations, ORNL/CDIAC-105, Carbon Dioxide Info. Anal. Cent., Oak Ridge Natl. Lab., US Dep. Of Energy, Oak Ridge, Tenn.

Llope M, Anadón R, Sostres JÀ, Viesca L (2007) Nutrients dynamics in the southern Bay of Biscay (1993-2003): Winter supply, stoichiometry, long-term trends, and their effects on the phytoplankton community. J Geophys Res C: Oceans 112: C07029, doi:10.1029/2006JC003573

Martin CL, Tortell PD (2006) Bicarbonate transport and extracellular carbonic anhydrase activity in Bering Sea phytoplankton assemblages: Results from isotope disequilibrium experiments. Limnol Oceanogr 51: 2111-2121

McGinn PJ, Morel FMM (2008) Expression and regulation of carbonic anhydrases in the marine diatom *Thalassiosira pseudonana* and in natural phytoplankton assemblages from Great Bay, New Jersey. Physiol Plant 133: 78-91

Mehrbach C, Culberson CH, Hawley JE, Pytkowicz RM (1973) Measurement of the apparent dissociation constants of carbonic acid in seawater at atmospheric pressure. Limnol Oceangr 18: 897-907.

Miller AG, Espie GS, Canvin DT (1988) Active transport of CO_2 by the cyanobacterium *Synechococcus* UTEX 625: measurement by mass spectrometry. Plant Biol 86: 677-683

Morel FMM, Cox EH, Kraepiel AML, Lane TW, Milligan AJ, Schaperdoth I, Reinfelder JR, Tortell PD (2002) Acquisition of inorganic carbon by the marine diatom *Thalassiosira weissflogii*. Funct Plant Biol 29: 301-308

Moroney JV, Husic HD, Tolbert NE (1985) Effect of carbonic anhydrase inhibitors on inorganic carbon accumulation by *Chlamydomonas reinhardtii*. Plant Physiol 79: 177-183

Nimer NA, Brownlee C, Merrett MJ (1994) Carbon dioxide availability, intracellular pH and growth rate of the coccolithophore *Emiliania huxleyi*. Mar Ecol Progr Ser 109: 257-262

Nimer NA, Dixon GK, Merrett MJ (1992) Utilization of inorganic carbon by the coccolithophorid *Emiliania huxleyi* (Lohmann) Kamptner. New Phytol 120: 153-158

Oguz T, Merico A (2006) Factors controlling the summer *Emiliania huxleyi* bloom in the Black Sea: A modeling study. J Mar Syst 59: 173-188

Ohlendieck U, Stuhr A, Siegmund H (2000) Nitrogen fixation by diazotrophic cyanobacteria in the Baltic Sea and transfer of the newly fixed nitrogen to picoplankton organisms. J Mar Syst 25: 213-219

Popp, B. , Laws, E., Bidigare, R., Dore, J., Hansen, K., Wakeham, S. (1998) Effect of phytoplankton cell geometry on carbon isotopic fractionation. *Geochimica y Cosmochimica Acta* 62, 69-77

Raven JA (1995) Costs and benefits of low intracellular osmolarity in cells of freshwater algae. Funct Ecol 9: 701-707

Raven JA (1997) CO_2-concentrating mechanisms: A direct role for thylakoid lumen acidification? Plant Cell Environ 20: 147-154

Raven JA (2010) Inorganic carbon acquisition by eukaryotic algae: four current questions. Photosynth Res 106: 123-134

Reinfelder JR (2011) Carbon concentrating mechanisms in eukaryotic marine phytoplankton. Annu Rev Mar Science 3: 291-315

Reinfelder JR, Kraepiel AML, Morel FMM (2000) Unicellular C4 photosynthesis in a marine diatom. Nature 407: 996-999

Reinfelder JR, Milligan AJ, Morel FMM (2004) The role of the C4 pathway in carbon accumulation and fixation in a marine diatom. Plant Physiol 135: 2106-2111

Riebesell U, Revill AT, Holdsworth DG, Volkman JK (2000) The effects of varying CO_2 concentration on lipid composition and carbon isotope fractionation in *Emiliania huxleyi*. Geochim Cosmochim Acta 64: 4179-4192

Riemann,B., Simonsen,P. and Stensgaard,L. (1989) The carbon and chlorophyll content of phytoplankton from various nutrient regimes. *J. Plankton Res*.11, 1037–1045.

Roberts K, Granum E, Leegood RC, Raven JA (2007) Carbon acquisition by diatoms. Photosynth Res 93: 79-88

Rost B, Kranz SA, Richter KU, Tortell PD (2007) Isotope disequilibrium and mass spectrometric studies of inorganic carbon acquisition by phytoplankton. Limnol Oceanogr: Methods 5: 328-337

Rost B, Riebesell U, Burkhardt S, Sültemeyer D (2003) Carbon acquisition of bloom-forming marine phytoplankton. Limnol Oceanogr 48: 55-67

Rost B, Riebesell U, Sültemeyer D (2006) Carbon acquisition of marine phytoplankton: Effect of photoperiod length. Limnol Oceanogr 51: 12-20

Spalding MH, Spreitzer RJ, Ogren WL (1983) Genetic and physiological analysis of the CO_2-concentrating system of *Chlamydomonas reinhardii*. Planta 159: 261-266

Spijkerman E (2011) The expression of a carbon concentrating mechanism in *Chlamydomonas acidophila* under variable phosphorus, iron, and CO_2 concentrations. Photosynth Research 109: 1-11

Suffrian K, Schulz KG, Gutowska MA, Riebesell U, Bleich M (2011) Cellular pH measurements in *Emiliania huxleyi* reveal pronounced membrane proton permeability. New Phytol 190: 595-608

Takahashi T, Sutherland SC, Sweeney C, Poisson A, Metzl N, Tilbrook B, Bates N, Wanninkhof R, Feely RA, Sabine C (2002) Global sea-air CO_2 flux based on climatological surface ocean pCO_2, and seasonal biological and temperature effects. Deep Sea Res Part II 49: 1601-1622

ter Kuile B, Erez J (1987) Uptake of inorganic carbon and internal carbon cycling in symbiont-bearing benthonic foraminifera. Mar Biol 94: 499-509

ter Kuile B, Erez J (1988) The size and function of the internal inorganic carbon pool of the foraminifer Amphistegina lobifera. Mar Biol 99: 481-487

Tortell PD (2000) Evolutionary and ecological perspectives on carbon acquisition in phytoplankton. Limnol Oceanogr 45: 744-750

Tortell PD, Martin CL, Corkum ME (2006) Inorganic carbon uptake and intracellular assimilation by subarctic Pacific phytoplankton assemblages. Limnol Oceanogr 51: 2102-2110

Tortell PD, Rau GH, Morel FMM (2000) Inorganic carbon acquisition in coastal Pacific phytoplankton communities. Limnol Oceanogr 45: 1485-1500

Trimborn S, Lundholm N, Thoms S, Richter KU, Krock B, Hansen PJ, Rost B (2008) Inorganic carbon acquisition in potentially toxic and non-toxic diatoms: The effect of pH-induced changes in seawater carbonate chemistry. Physiol Plant 133: 92-105

Trimborn S, Wolf-Gladrow D, Richter KU, Rost B (2009) The effect of pCO_2 on carbon acquisition and intracellular assimilation in four marine diatoms. J Exper Mar Biol Ecol 376: 26-36

UNESCO (1994) Protocols for the Joint Global Ocean Flux Study (JGOFS) core measurements, IOC/SCOR manual and guides. UNESCO Publ 29: 128-134

Wannicke N, Koch BP, Voss M (2009) Release of fixed N_2 and C as dissolved compounds by *Trichodesmium erythreum* and *Nodularia spumigena* under the influence of high light and high nutrient (P). Aquat Microb Ecol 57: 175-189

Woodger FJ, Badger MR, Price GD (2003) Inorganic carbon limitation induces transcripts encoding components of the CO_2-concentrating mechanism in *Synechococcus* sp. PCC7942 through a redox-independent pathway. Plant Physiol 133: 2069-2080

FIGURE LEGENDS:

Fig. 1. Idealized model for detecting the C_i pool during a pulse-chase experiment. The solid black line represents the ^{14}C uptake during the pulse, the dotted line represents increased ^{14}C in the algae during the chase period. This ^{14}C is transferred from the C_i pool into the particulate organic matter and serves as an estimate of the C_i pool. The dashed line indicates the loss of ^{14}C within the particulate organic matter due to respiration.

Fig. 2. DIC incorporation rates measured during the pulse incubation (n=3). a – *T. weissflogii*. b – *E. huxleyi*.

Fig. 3. Pulse-chase experiments illustrating acid-labile C_i pools at 3 different pH settings of *T. weissflogii*. Cells were spiked with ^{14}C and the kinetics of acid-stable photosynthetic products were followed for 120 min (pulse) after which the cells were resuspended in label-free medium under identical experimental conditions (chase). Each datapoint reflects 3 single measurements. a – Culture preincubated at a pH of 8.5 b – Culture preincubated at a pH of 7.9. c – Culture preincubated at a pH of 7.4. The different symbols represent the repetitions of the experiment.

Fig. 4. Pulse-chase experiments illustrating acid-labile C_i pools at 3 different pH settings of *E. huxleyi*. Cells were spiked with ^{14}C and the kinetics of acid-stable photosynthetic products were followed for 120 min (pulse) after which the cells were resuspended in label-free medium under identical experimental conditions (chase). Each datapoint reflects 3 single measurements. a – Culture preincubated at a pH of 8.5 b – Culture preincubated at a pH of 7.9. c – Culture preincubated at a pH of 7.4. The different symbols represent the repetitions of the experiment.

Fig. 5. C_i pool size variation related to differences in the carbon system (n=3). a – *T. weissflogii* C_i pool vs. pH. b – *T. weissflogii* C_i pool vs. $CO_{2(aq)}$. c– *T. weissflogii* C_i pool vs.

DIC. d – *E. huxleyi* C_i pool vs. pH. e – *E. huxleyi* C_i pool vs. $CO_{2(aq)}$. f– *E. huxleyi* C_i pool vs. DIC.

Fig. 6. a – *T. weissflogii* Chl*a* vs. pH. b – *T. weissflogii* C_i pool vs. Chl*a*. c – *T. weissflogii* Chl*a*:cell volume vs. pH. d – *E. huxleyi* Chl*a* vs. pH. e – *E. huxleyi* C_i pool vs. Chl*a*. c – *E. huxleyi* Chl*a*:cell volume vs. pH. (n=3).

Fig. 7. Results from ^{14}C disequilibrium assays for *E. huxleyi* and *T. weissflogii* at different pH levels. a - *T. weissflogii* at pH 7.49. b - *T. weissflogii* at pH 7.90. c - *E. huxleyi* at pH 7.49, (d) *E. huxleyi* at pH 7.82. e - *E. huxleyi* at pH 8.11, Solid lines and filled circles represent samples without any inhibition, dashed lines and empty circles represent DBS inhibition (50 µmol L^{-1}) during the sampling Values of *f* denote the proportion of HCO_3^- to DIC fixation in non-treated (control) and DBS treated cells. Values and standard deviations are based on triplicate measurements.

Fig. 8. Ratio of gross CO_2 : HCO_3^- uptake in *T. weissflogii* and *E. huxleyi* with respect to different pCO_2 values. Data of shaded bars were obtained during this study, remaining data were published by Burkhardt et al. (2001) for *T. weissflogii* and by Rost et al (2003) for *E. huxleyi*. Values and standard deviations are based on triplicate measurements. The dashed line indicates the value when CO_2 and HCO_3^- are taken up in equal proportions.

886

Table 1. ^{14}C experimental data of the added activity of ^{14}C during the pulse incubation (AA), measured blanks = time zero values (TZ), TZ relative to AA, average (n=5) or single measurements of chase added activity of ^{14}C (CA) measured during the chase, CA relative to AA, measured ^{14}C activity on the filter after washing (CF), equivalent culture volume of CF with respect to the maximum measurement during the pulse incubation.

Species	pH	AA [CPM mL^{-1}]	TZ [CPM mL^{-1}]	TZ : AA [‰]	CA [CPM mL^{-1}]	CA :AA [‰]	CF [CPM]	CF equivalent V [mL]
T. weissflogii	8.35	479,930	9.00	0.02	3029	6.20	4,218	2.4
	8.62	156,460	7.00	0.05	221 ± 11	1.36	1,065	1
	8.56	60,543	5.00	0.09	454 ± 25	8.10	1,404	5.7
	7.94	772,222	109.00	0.10	326	0.42	7,596	0.6
	7.99	127,393	8.00	0.10	731 ± 48	5.70	560	0.4
	7.94	64,700	4.00	0.10	295 ± 23	4.70	392	1.3
	7.47	297,610	7.00	0.02	488	1.64	1,756	1.5
	7.47	74,433	4.00	0.05	347 ± 10	4.79	264	3.4
	7.47	73,025	3.00	0.04	348 ± 19	4.71	602	2.5

E. huxleyi	8.47	210,965	13.00	0.06	304	1.44	1,721	2.2
	8.43	54,300	3.00	0.06	460 ± 15	8.55	293	6.1
	8.36	70,770	3.00	0.04	587 ± 26	8.67	600	11.8
	7.96	70,715	4.00	0.06	245 ± 15	3.42	921	7.4
	7.96	76,295	4.00	0.05	237 ± 35	3.13	313	4.7
	7.91	56,168	3.32	0.06	333 ± 23	6.28	518	10.7
	7.45	261,355	18.00	0.07	345	1.32	2,112	4.6
	7.44	61,468	3.00	0.06	353 ± 21	5.18	214	14.0
	7.47	65,800	5.00	0.08	530 ± 20	8.75	221	16.0

Table 2. Comparison of the light (L) and the dark (D) C_i incorporation rate per cell.

Species	pH	L	D	D:L C_i incorporation [%]
		C_i incorporation rate *T. weissflogii* [pmol C_i h^{-1} $cell^{-1}$] *E. huxleyi* [pmol C_i h^{-1} $cell^{-1}$]		
T. weissflogii	8.35	1.76	0.03	1.44
	7.47	2.52	0.06	2.42
E. huxleyi	8.47	0.003	0.00003	1.00
	7.97	0.018	0.000009	0.5

Table 3. Measured pH values of the media, cell concentrations, cell volumes, Chl*a* concentrations, C_i uptake rates, average C_i pools (n=3), internal C_i concentrations, ratio of internal to external C_i concentrations.

Species	pH	TA [µmol kg SW^{-1}]	$C_{i\ ext}$ [µmol kg SW^{-1}]	$CO_{2(aq)}$ [µmol kg SW^{-1}]	pCO_2 [µatm]	cells [cells ml^{-1}]	V_{cell} [μm^3]	Chl*a* [pg $cell^{-1}$]	C_i uptake rate [pmol DIC h^{-1} $cell^{-1}$]	C_i pool [pmol $cell^{-1}$]	$C_{i\ int}$ [mmol L^{-1}]	C_i int: ext
T. weissflogii	8.35	2,613	2,219	9.2	269	21,258			1.76	0.522 ± 0.268	5.44	2.5
	8.62	1,420	1,019	2.0	60	16,750	960	7.58	4.34	1.399 ± 1.027	14.56	14.3
	8.56	3643	2,919	6.8	201	8,111	1,229	7.06	6.40	2.133 ± 0.745	17.36	7.6
	7.94	2,550	2,394	27.3	804	35,970			4.95	0.891 ± 0.190	7.40	3.1
	7.9	2,880	2,687	27.3	804	14,600	1,203	8.49	9.25	1.419 ±	11.79	4.4

	9								1.405		
	7.94	2,270	2,125	24.3	715	9,900	2,098	7.27	5.04	0.490 ± 0.477	2.34	1.1
	7.47	1,540	1,543	52.6	1,548	13,860			0.20	0.018 ± 0.034	0.00	0.0
	7.47	1,837	1,843	62.3	1,833	3,600	1,044	4.56	2.52	0.027 ± 0.019	0. 26	0.1
	7.47	2,467	2,485	84.7	2,494	7,800	1,233	5.01	4.92	0.0 ± 0.819	0. 00	0.0
E. huxleyi	8.47	2,590	2,110	6.4	187	163,100			3.00E-03	6.284E-03 ± 2.456E-03	3.45	1.6
	8.43	1,873	1,514	5.1	149	98,900	18.2	0.057	6.00E-03	3.113E-03 ± 1.214E-	1.65	1.1

8.36	1,450	1,177	4.7	138	75,800	17.8	0.082	6.00E-03	03 4.319E-03 ± 4.109E-03	2.42	2.1
7.96	1,613	1,487	16.1	472	106,400	28.2	0.047	1.80E-02	1.267E.03 ± 2.303E-04	0. 74	0.3
7.96	1,953	1,812	19.6	576	69,798	17.6	0.116	1.20E-02	1.34E-03 ± 8.168E-04	0. 91	0.5
7.91	2,773	2,622	32.1	946	76,200	31.5		1.80E-02	1.941E-03 ± 1.349E-	0. 62	0.2

									03		
7.45	1,350	1,354	48.3	1,422	120,270			1.20E-03	0.0 ± 1.478E-04	0.00	0.0
7.47	937	9,35	34.5	1,015	90,900	23.7	0.011	1.80E-03	0.0 ± 2.33E-04	0.00	0.0
7.47	2,107	2,120	72.9	2,146	89,400	37.7	0.033	3.00E-03	1.291E-04 ± 7.212E-04	0.03	0.0

Table 4. Intracellular DIC concentrations, obtained with different methods, of different species and the corresponding external DIC concentration, respectively $CO_{2(aq)}$ concentration, as well as the ratio of surface area (SA) and volume (V)of the single cells (SOC – silicon oil centrifugation method; MIMS – mass spectrometry analysis; P+C – pulse chase method).

Species	Source	Method	$C_{i\ int}$ [mmol L^{-1}]	$C_{i\ ext}$ [mmol L^{-1}]	$C_{i\ int}$: $C_{i\ ext}$	SA:V
E. huxleyii	Nimer et al. 1994	SOC	0.1-0.32	0.1-1	1-15	
	Nimer et al. 1992	SOC	0.05-0.35	0.1-1	1-15	
	Dong et al. 1993	SOC	0.015-0.04	0.01-0.1	1-15	
	This study	P+C	0.6-3.5	1.1-2.5	0.2-2.1	1.8
T. weissflogii	This study	P+C	2.4-17.4	1-2.6	1.1-14.3	0.5
Phaeodactylum tricornutum	Burns and Beardall 1987	MIMS	0.99	0.15	5-6	2.6
	Dixon and Merrett 1988	MIMS	0.5-1.8	0.1-0.5	5-6	

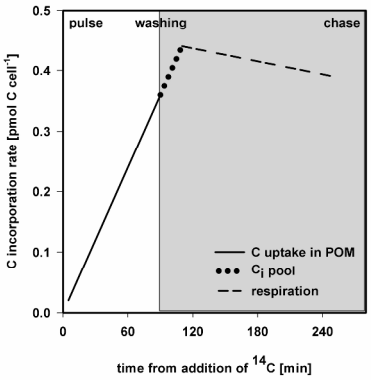

Fig. 1. Idealized model for detecting the Ci pool during a pulse-chase experiment. The solid black line represents the 14C uptake during the pulse, the dotted line represents increased 14C in the algae during the chase period. This 14C is transferred from the Ci pool into the particulate organic matter and serves as an estimate of the Ci pool. The dashed line indicates the loss of 14C within the particulate organic matter due to respiration.
296x420mm (300 x 300 DPI)

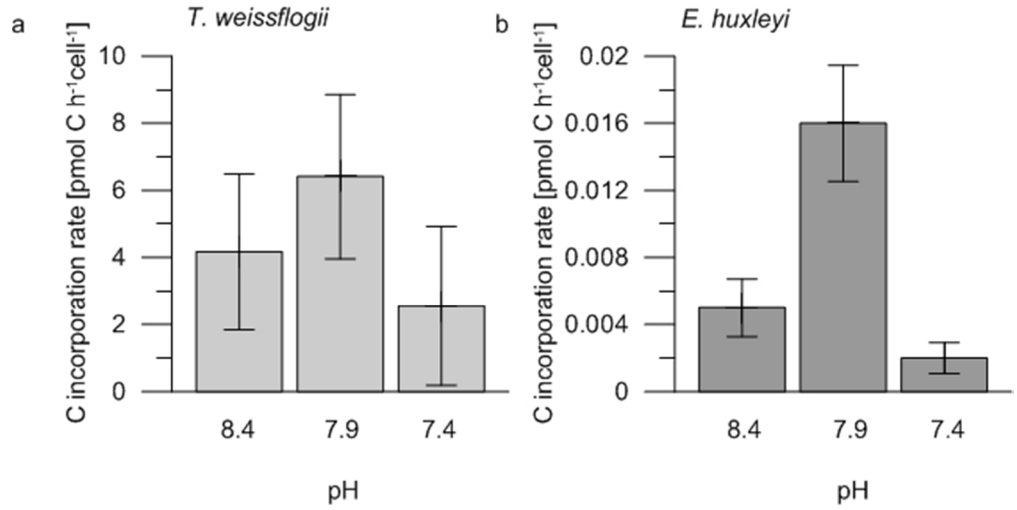

Fig. 2. Ci incorporation rates measured during the pulse incubation (n=3). a – T. weissflogii. b – E. huxleyi.
169x85mm (96 x 96 DPI)

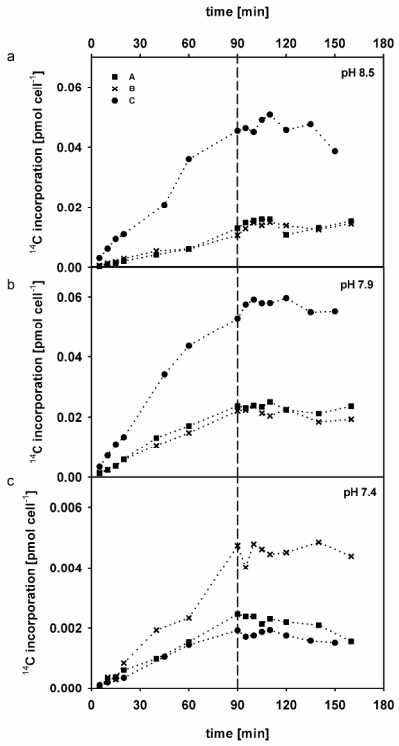

Fig. 3. Pulse-chase experiments illustrating internal Ci pools at 3 different pH settings of T. weissflogii. Cells were spiked with 14C and the kinetics of acid-stable photosynthetic products were followed for 120 min (pulse) after which the cells were resuspended in label-free medium under identical experimental conditions (chase). Each datapoint reflects the average of 3 filters measured for 14C activity from the same culture. Different symbols are from replicate culture incubations under similar pH conditions A, B, C. a – Culture preincubated at a pH of 8.5 b – Culture preincubated at a pH of 7.9. c – Culture preincorporated at a pH of 7.4.
296x420mm (300 x 300 DPI)

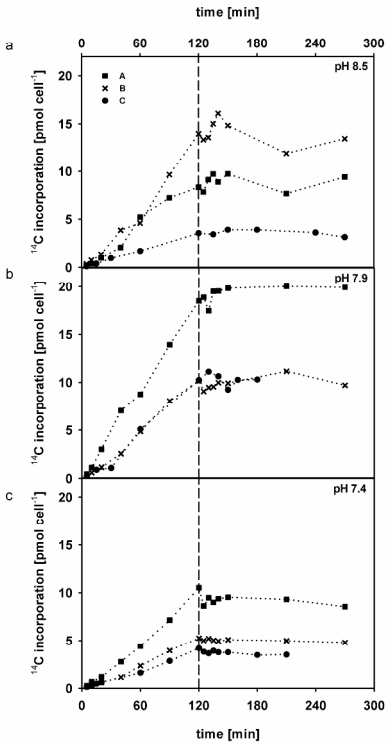

Fig. 4. Pulse-chase experiments illustrating internal Ci pools at 3 different pH settings of E. huxleyi. Cells were spiked with 14C and the kinetics of acid-stable photosynthetic products were followed for 120 min (pulse) after which the cells were resuspended in label-free medium under identical experimental conditions (chase). Each datapoint reflects the average of 3 filters measured for 14C activity from the same culture. Different symbols are from replicate culture incubations under similar pH conditions A, B, C.a – Culture preincubated at a pH of 8.5 b – Culture preincubated at a pH of 7.9. c – Culture preincorporated at a pH of 7.4.
296x420mm (300 x 300 DPI)

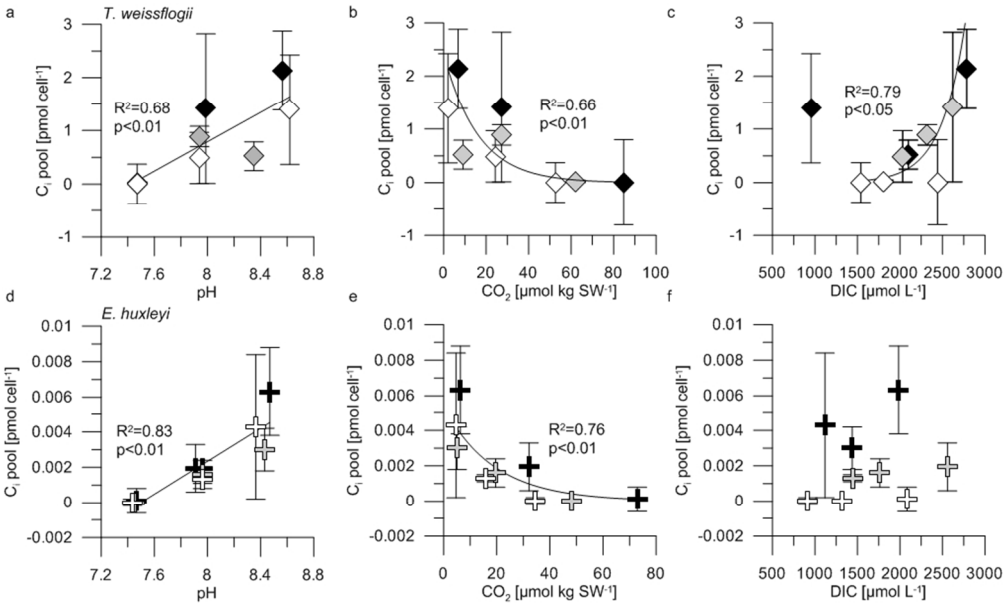

Fig. 5. Ci pool size variation related to differences in the carbon system (n=3). White symbols – lowest DIC values (a, d), lowest pH levels (c, f); grey symbols – intermediate Ci values (a, d), intermediate pH levels (c, f); black symbols – high Ci values (a, d), high pH levels (c, f). a – T. weissflogii Ci pool vs. pH. b – T. weissflogii Ci pool vs. CO2(aq). c– T. weissflogii Ci pool vs. DIC. d – E. huxleyi Ci pool vs. pH. e – E. huxleyi Ci pool vs. CO2(aq). f– E. huxleyi Ci pool vs. DIC.
268x161mm (96 x 96 DPI)

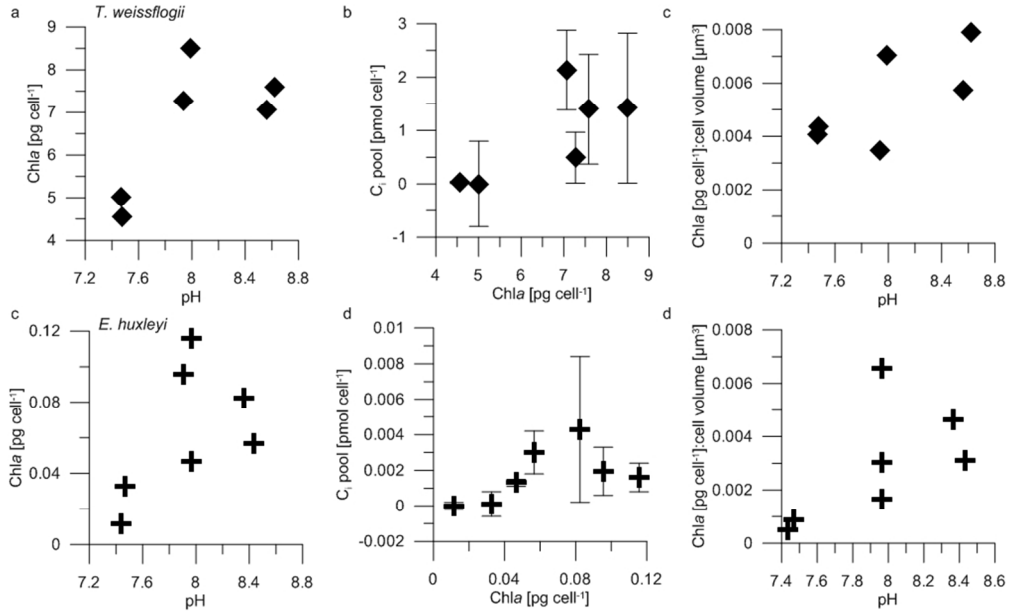

Fig. 6. a – T. weissflogii Chla vs. pH. b – T. weissflogii Ci pool vs. Chla. c – T. weissflogii Chla:cell volume vs. pH. d – E. huxleyi Chla vs. pH. e – E. huxleyi Ci pool vs. Chla. c – E. huxleyi Chla:cell volume vs. pH. (n=3). 266x161mm (96 x 96 DPI)

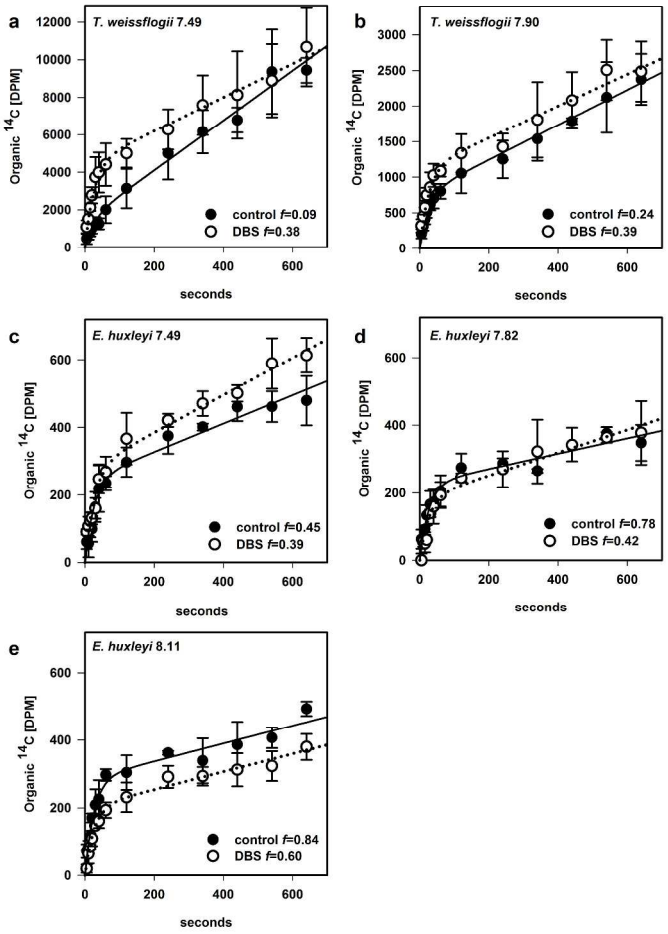

Results from 14C disequilibirum assays for E. huxleyi and T. weissflogii at different pH levels. a - T. weissflogii at pH 7.49. b - T. weissflogii at pH 7.90. c - E. huxleyi at pH 7.49, (d) E. huxleyi at pH 7.82. e - E. huxleyi at pH 8.11, Solid lines and filled circles represent samples without any inhibition, dashed lines and empty circles represent DBS inhibition (50 µmol L-1) during the sampling Values of f denote the proportion of HCO3- to C fixation in non treated (control) and DBS treated cells. Values and standard deviations are based on triplicate measurements.
296x420mm (300 x 300 DPI)

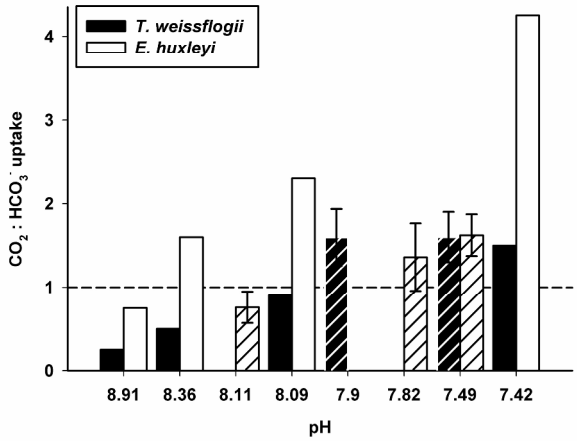

Ratio of gross CO2 : HCO3- uptake in T. weissflogii and E. huxleyi with respect to different pCO2 values. Data of shaded bars were obtained during this study, remaining data were published by Burkhardt et al. (2001) for T. weissflogii and by Rost et al (2003) for E. huxleyi. Values and standard deviations are based on triplicate measurements. The dashed line indicates the value when CO2 and HCO3- are taken up in equal proportions.
296x420mm (300 x 300 DPI)